Observation of Associative Ionization of Ultracold Laser-Trapped Sodium Atoms

P. L. Gould,[a] P. D. Lett,[a] P. S. Julienne,[b] and W. D. Phillips[a]
National Bureau of Standards, Gaithersburg, Maryland 20899

and

H. R. Thorsheim and J. Weiner
Department of Chemistry, University of Maryland, College Park, Maryland 20742
(Received 17 December 1987)

We have observed associative ionization of laser-cooled and -trapped sodium atoms. The measured rate coefficient for the process at a temperature of 0.75 ± 0.25 mK is $(1.1^{+1.3}_{-0.3}) \times 10^{-11}$ cm^3 s^{-1}, which implies a cross section of 8.6×10^{-14} cm^2. This is 3 orders of magnitude larger than the cross section measured in previous experiments at higher temperatures. The measurement involves the use of a new kind of laser trap.

PACS numbers: 32.80.Pj, 34.50.−s, 34.50.Rk

Recent advances[1-6] in laser cooling and trapping of neutral atoms have paved the way for experiments using the resulting cold, dense atomic gases. In this Letter, we present the first observation, identification, and measurement of a specific collisional process in such a unique sample. This low-energy regime is novel for several reasons: (1) Collisions can be highly nonclassical. When the de Broglie wavelength of the collision partners is long relative to the range of the interaction potentials, a semiclassical, trajectory treatment is inappropriate. (2) Only a small number of partial waves contribute to the collision cross section. (3) The collision dynamics can be dominated by weakly attractive, long-range potentials which are unimportant at high collision energies.

We study the associative ionization (AI) reaction

$$Na^* + Na^* \rightarrow Na_2^+ + e^-, \quad (1)$$

where $Na^* = Na(3P_{3/2})$. The AI process has been studied extensively with vapor cells[7] and atomic-beam techniques.[8,9] Those experiments, however, were limited to collision energies greater than 20 K. We measure the AI cross section for ultracold (0.75 mK) excited sodium atoms to be 8.6×10^{-14} cm^2, a value approximately 3 orders of magnitude larger than that measured at collision velocities corresponding to energies ranging from 2400 to 20 K.[8] The large value of this cross section implies, as Vigue has suggested,[10] that collisional processes will be important factors in limiting the atomic densities achievable with laser-cooling and -trapping techniques.

The experiment is performed with sodium atoms which are laser cooled and confined in a novel, hybrid laser trap. This trap, based on Ashkin's proposal,[11] uses both the spontaneous-radiation pressure force and the dipole force for confinement; it will be described in detail in a future publication. The trap (see Fig. 1) has two counterpropagating, circularly polarized (σ^+), Gaussian laser beams brought to separate foci. With the laser tuned below resonance, radial confinement is provided by the dipole force. Axial confinement about the midpoint between the foci results from the differential spatial variation in the radiation pressure from the two beams. Following a suggestion by Dalibard and Cohen-Tannoudji,[12] the two beams are alternated in time to avoid the large dipole heating[13] that results from the presence of standing waves. The trapping periods are alternated with Doppler cooling periods[14] which serve to damp the atomic motion.

The trap is embedded in a much larger (~ 1 cm diam) region of two-frequency "optical molasses"[2,5] formed at the intersection of three pairs of counterpropagating, collimated laser beams. This molasses captures and confines slow atoms emanating continuously from a laser-cooled atomic beam,[15] allowing us to achieve steady-state total densities of $\simeq 10^7$ atoms/cm^3 at temperatures near the cooling limit (240 μK for sodium). Atoms from the molasses are captured by the trap and are compressed to a much higher density. As pointed out by Chu *et al.*,[4] the optical molasses is ideal for loading the trap and maintaining a low temperature.

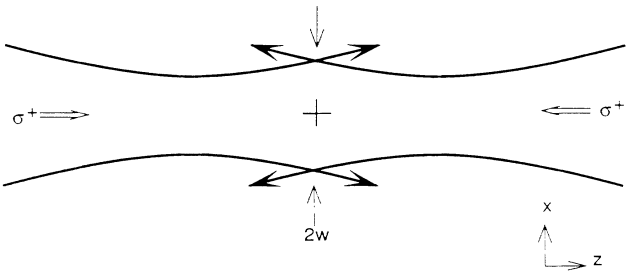

FIG. 1. Laser-trap geometry (not to scale). Foci of the two beams are separated by about the confocal parameter. Stable trapping is achieved at the midpoint between the foci (shown as a cross) where the waist ($1/e^2$ radius of intensity) is w.

Typically, each trap beam has a power of $\simeq 40$ mW and is focused to produce a waist ($1/e^2$ radius of intensity) of $w \simeq 100$ μm at the trap center. At a detuning of approximately -700 MHz [relative to the $(3S_{1/2}, F=2) \rightarrow (3P_{3/2}, F'=3)$ transition], the time-averaged radial well depth is $\simeq 10$ mK. The axial depth (to each focus) is much larger: we estimate it to be on the order of a kelvin. Each trap beam is on for 3 μs and trapping periods are alternated with 3-μs cooling periods. The effect of the molasses (cooling) beams is turned off by the large ac Stark shifts when a trap beam is on.

Excitation to the $3P_{3/2}$ state (necessary for AI) occurs during both trapping and cooling periods. We calculate that while a trap beam is on, the atom spends $\simeq 35\%$ of its time in the excited state, cycling between $F=2$, $m_F=2$ and $F'=3$, $m_{F'}=3$. The six molasses beams typically have an intensity of $\simeq 14$ mW/cm^2 each and are detuned $\simeq 10$ MHz below the $F=2 \rightarrow F'=3$ transition, resulting in a calculated excited-state fraction of $\simeq 13\%$ during the "trap-off" cooling period. These three orthogonal pairs of beams have orthogonal linear polarizations so that the trapped atoms are assumed to be equally distributed among the various m states during cooling.

Fluorescence from excited atoms in the trap is collected and imaged with a calibrated charge-coupled-device video camera. The spatial resolution of the optical system, measured as the FWHM of the δ-function response, is $\simeq 12$ μm at the trap. The spatial distribution of excited atoms is determined from the video image and is typically 40 μm FWHM radially and 800 μm axially. The three-dimensional excited-state density profile is derived from the two-dimensional image by the assumption of a Maxwellian atomic velocity distribution. This implies that the distribution of excited atoms is Gaussian in the harmonic (central) portion of the trap. From the radial distribution of atoms and the calculated trap potential, we determine the temperature to be 0.75 ± 0.25 mK.

Ions formed in the trap are accelerated into a Johnston model MM1 focused-mesh electron multiplier[16] and counted. In order to determine the mass of the ions, we have measured the time-of-flight mass spectrum which results when a pulsed electric field is used to extract ions which accumulate over many trapping-cooling cycles. A typical spectrum is shown in Fig. 2. The ions are predominantly Na_2^+; our signal-to-noise ratio allows us to determine that the Na^+ fraction is less than 20%.

In order to verify that the Na_2^+ is produced in a binary Na-Na collision process, we have measured the dependence of the ion production rate on the density of trapped excited atoms. The density is varied by our changing the flux of slow atoms which enter the molasses and load the trap. The parameters of the molasses and the trap are held fixed in an attempt to maintain the same density profile and temperature in the trap, and so the total fluorescence from the trap is assumed to be directly proportional to the density of excited atoms. Data taken in this manner are shown in Fig. 3. When plotted on a log-log scale, data for a two-body collisional process should yield a straight line with a slope of 2.0. Some of the data on ion rate versus fluorescence suggest a decreasing slope at higher densities. (While the data are not sufficiently accurate to confirm this, we may speculate that collisional loss processes, e.g., collisional heating,[17] are responsible for such a trend. These processes, being more rapid in regions of high density, could cause distortions in the trap density profiles.) Nevertheless, the data support the hypothesis that the ions are formed in binary Na-Na collisions.

Measurement of the absolute AI rate coefficient K requires absolute determinations of ion production rate and

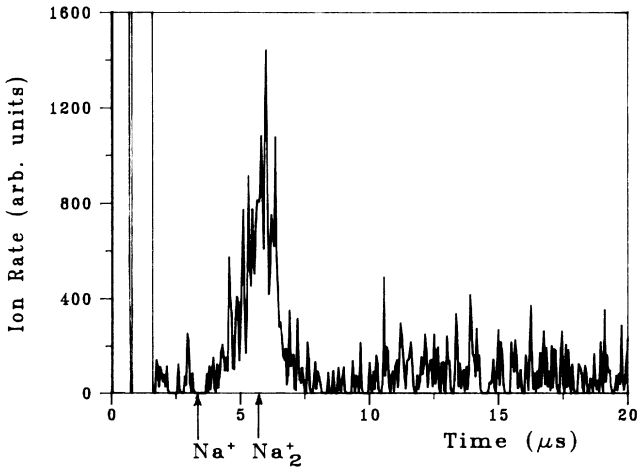

FIG. 2. Time-of-flight mass spectrum of ions produced in the laser trap. Arrows indicate the calculated arrival times for Na^+ and Na_2^+. The large signal at short times is due to ringing of the high-voltage pulse.

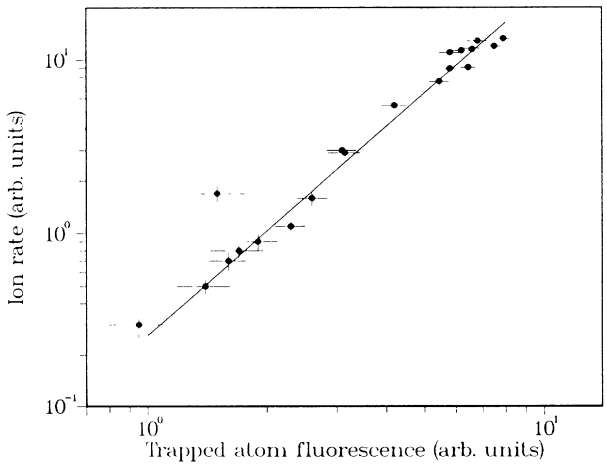

FIG. 3. Log-log plot of ion signal vs trapped-atom fluorescence (arbitrary units). The solid line has a slope of 2.0. Error bars represent random fluctuations in the measurement of a single point.

excited-state density. These quantities are measured as the difference between conditions with and without the trap in order to eliminate small background contributions. The "without trap" condition is achieved by our detuning the trap laser, keeping the power constant. The ion rate is measured by counting with an ion collection and detection system whose efficiency is assumed to be 90% (on the basis of the specified multiplier efficiency and the geometry). We obtain the absolute density from a combination of absolute excited-atom number measurements (using both the calibrated camera and a calibrated photomultiplier tube to measure total trap fluorescence) and measurements of the density profile (using the video image). The ion production rate, dN_I/dt, is related[18] to the excited-state density, n_e, according to

$$DN_I/dt = K\int n_e^2(\mathbf{r})d^3r = K\bar{n}_e N_e, \tag{2}$$

where $\bar{n}_e$ is the effective trap density and N_e is the total number of excited atoms in the trap: $N_e = \int n_e(\mathbf{r})d^3r$.

We typically observe a steady-state $dN_I/dt = 1.1\times10^3$ ions/s with $N_e = 2.0\times10^4$ excited atoms in an effective volume of 4.0×10^{-6} cm^3, implying $\bar{n}_e = 5.0\times10^9$ cm^{-3}. This yields a rate coefficient of $K = (1.1^{+1.3}_{-0.5})\times10^{-11}$ cm^3 s^{-1}.[18] The uncertainty in this value comes mainly from the determination of $n_e(\mathbf{r})$. If we assume an average collision velocity of 130 cm s^{-1} (i.e., a temperature of 0.75 mK), this gives a cross section of $\sigma = (8.6^{+10.0}_{-3.8})\times10^{-14}$ cm^2. By contrast, the cross section at a velocity corresponding to an energy of 20 K has been measured[8] to be about 10^{-16} cm^2 and is decreasing with decreasing temperature.

The basic physical problem we must address is how the cross section can be so large at these ultralow temperatures. To appreciate the novel effects of ultracold atom collisions we must understand the specific quantum threshold behavior due to the long-range approach of the two atoms. If we neglect the effect of multiple entrance channels, the quantum-mechanical integral cross section for inelastic scattering from entrance channel 1 to the AI exit channel 2 has the form

$$\sigma_{12}(\epsilon) = (\pi/k^2)\sum_{l=0}^{\infty}(2l+1)\,|S_{12}(\epsilon,l)|^2$$

$$\cong \pi\lambda\!\!\!^{-2}(l_{\max}+1)^2 P_{12} \tag{3}$$

for center-of-mass collision energy $\epsilon = \hbar^2k^2/2\mu$, reduced mass μ, and relative angular momentum l. The quantity $|S_{12}(\epsilon,l)|^2$ represents the inelastic scattering probability, for which the unitarity of the S matrix gives an upper limit of 1. In the second expression in (3), $\lambda\!\!\!^{-} = 1/k = \lambda/2\pi$, where λ is the entrance-channel de Broglie wavelength, and P_{12} represents the mean probability of AI averaged over contributing partial waves whose maximum angular momentum is $l_{\max}$.

Even if we assume that only s waves ($l_{\max}=0$) contribute in our case ($\epsilon = \frac{3}{2}k_BT$ with $T = 0.75$ mK, for which $\lambda\!\!\!^{-} = 4.3$ nm) we get an upper limit of 9×10^{-13} cm^2 for the cross section. Thus the large measured value does not violate the s-wave unitarity condition. Note that for large $l_{\max}$, $\lambda\!\!\!^{-}l_{\max} = b_{\max}$, where $b_{\max}$ is the classical impact parameter. For high-temperature collisions (700 K) $b_{\max}$ has been measured to be about 0.2 nm, and P_{12} is about 0.1.[19] On the other hand, $\lambda\!\!\!^{-}(l_{\max}+1)$ at 0.75 mK is $\geqq 4.3$ nm, depending on the magnitude of $l_{\max}$. If $l_{\max}\geqq 1$, then the measured cross section at 0.75 mK implies that P_{12} is actually much smaller at 0.75 mK than at 700 K. We conclude that the large measured cross section is not unreasonable. It is a consequence of the large value of λ for near-threshold collisions.

We have carried out quantum-mechanical calculations to simulate the entrance-channel threshold behavior for realistic long-range R^{-n} potentials. The details of this analysis will be described elsewhere. It is necessary to take into account both the long-range R^{-5} quadrupole-quadrupole interaction with which two excited $3P_{3/2}$ atoms approach one another and the modification of the long-range potential due to interaction of the asymptotic atoms with the strong radiation field for collisions which occur when the strong trapping laser is on. Both aspects of the potential are sensitive to atomic orientation. The physics of the collision can be separated into two distinct regions: the asymptotic long-range region in which the approach of the two atoms is governed by the attractive or repulsive nature of the long-range potential and a short-range region in which AI occurs. The short-range physics is essentially independent of the asymptotic physics. The important role of the asymptotic region is to control how many partial waves l contribute to the sum in (3) as a result of small centrifugal barriers in the approach of the two atoms on an attractive potential.

We note that AI can be an important loss mechanism for laser traps. Under our typical conditions, it contributes a decay rate of 0.03 s^{-1}. Inelastic collisions between ground- and excited-state atoms (collisional heating) are predicted[17] to lead to even higher loss rates. With improved loading (leading to higher density), the lifetime in the trap will become dominated by these collisional loss mechanisms (as opposed to loss due to collisions with background gas) and will eventually cause the steady-state density to increase only with the square root of the loading rate. Prentiss *et al.*[20] have reported a density-dependent loss rate for a different kind of laser trap,[1] which implies a rate constant of 4×10^{-11} cm^3 s^{-1}. It is independent of the excited-state fraction, and therefore cannot be due to AI.

In conclusion, we have made the first measurement of a collision process at a submillikelvin temperature and the first application of laser-cooled neutral atoms to study a previously inaccessible physical regime. With these techniques, it will be possible to investigate other

collisional processes: photoassociation,[21] collisional heating,[17] state-changing collisions, and cluster formation. The large size of this cross section at low temperature has important consequences for the achievement of high densities of neutral atoms with use of laser cooling and trapping techniques.

We are grateful for financial support from the Office of Naval Research and the National Science Foundation. One of us (P.L.G.) is a National Research Council–National Bureau of Standards Postdoctoral Fellow.

---

[a]Electricity Division, Center for Basic Standards.

[b]Molecular Spectroscopy Division, Center for Chemical Physics.

[1]E. L. Raab, M. Prentiss, A. Cable, S. Chu, and D. E. Pritchard, Phys. Rev. Lett. **59**, 2631 (1987).

[2]P. L. Gould, P. D. Lett, and W. D. Phillips, in *Laser Spectroscopy VIII,* edited by S. Svanberg and W. Persson (Springer-Verlag, Berlin, 1987), p. 64.

[3]V. S. Bagnato *et al.*, Phys. Rev. Lett. **58**, 2194 (1987).

[4]S. Chu, J. E. Bjorkholm, A. Ashkin, and A. Cable, Phys. Rev. Lett. **57**, 314 (1986).

[5]S. Chu, L. Hollberg, J. E. Bjorkholm, A. Cable, and A. Ashkin, Phys. Rev. Lett. **55**, 49 (1985).

[6]A. L. Migdall *et al.*, Phys. Rev. Lett. **54**, 2596 (1985).

[7]J. Huennekens and A. Gallagher, Phys. Rev. A **28**, 1276 (1983); V. S. Kushawaha and J. J. Leventhal, Phys. Rev. A **22**, 2468 (1980); A. Klyucharev, V. Sepman, and V. Vuinovich, Opt. Spectrosc. **42**, 336 (1977).

[8]R. Bonanno, J. Boulmer, and J. Weiner, Comments At. Mol. Phys. **16**, 109 (1985); M.-X. Wang, J. Keller, J. Boulmer, and J. Weiner, Phys. Rev. A **35**, 934 (1987), and **34**, 4497 (1986).

[9]A. deJong and F. van der Valk, J. Phys. B **12**, L561 (1979); H. A. J. Meijer, H. P. van der Meulen, and R. Morgenstern, Z. Phys. D **5**, 299 (1987), and references therein.

[10]J. Vigue, Phys. Rev. A **34**, 4476 (1986).

[11]A. Ashkin, Phys. Rev. Lett. **40**, 729 (1978).

[12]J. Dalibard and C. Cohen-Tannoudji, private communication.

[13]J. P. Gordon and A. Ashkin, Phys. Rev. A **21**, 1606 (1980).

[14]J. Dalibard, S. Reynaud, and C. Cohen-Tannoudji, Opt. Commun. **47**, 395 (1983).

[15]W. D. Phillips, J. V. Prodan, and H. J. Metcalf, J. Opt. Soc. Am. B **2**, 1751 (1985).

[16]Specification of an item by brand name is for identification purposes only and does not constitute an endorsement by the National Bureau of Standards.

[17]H. R. Thorsheim, J. Weiner, S. H. Pan, and P. S. Julienne, to be published.

[18]Our calculations of the rate coefficient uses a measured excited-state density which is time averaged over trapping and cooling periods. We ignore differences in density and rate coefficient between these periods.

[19]J. Keller, R. Bonanno, M. X. Wang, M. S. de Vries, and J. Weiner, Phys. Rev. A **33**, 1612 (1986).

[20]M. Prentiss, A. Cable, J. E. Bjorkholm, and S. Chu, to be published.

[21]H. R. Thorsheim, J. Weiner, and P. S. Julienne, Phys. Rev. Lett. **58**, 2420 (1987).